

Shape and coarsening dynamics of strained islands

Guido Schifani,¹ Thomas Frisch,^{1,*} Mederic Argentina,¹ and Jean-Noël Aqua²

¹*Université Côte d'Azur, CNRS, INLN, France*

²*Université Paris VI, CNRS, INSP, France*

We investigate the formation and the coarsening dynamics of islands in a strained epitaxial semiconductor film. These islands are commonly observed in thin films undergoing a morphological instability due to the presence of the elasto capillary effect. We first describe both analytically and numerically the formation of an equilibrium island using a two dimensional continuous model. We have found that these equilibrium island-like solutions have a maximum height h_0 and they sit on top of a flat wetting layer with a thickness h_w . We then consider two islands and we report that they undergo a non-interrupted coarsening that follows a two stage dynamics. The first stage may be depicted by a quasi-static dynamics, where the mass transfers are proportional to the chemical potential difference of the islands. It is associated with a time scale t_c that is function of the distance d between the islands, and leads to the shrinkage of the smallest island. Once its height becomes smaller than a minimal equilibrium height h_0^* , its mass spreads over the entire system. Our results pave the way for a future analysis of coarsening of an assembly of islands.

PACS numbers: 81.15.Hi, 68.35.Ct, 81.10.Aj, 47.20.Hw

Understanding the dynamics of coarsening and its effect on self-organisation is a central question in non-equilibrium physics and solid-state physics since its experimental discovery by Ostwald at the end of the 19th century [1] and the seminal theoretical papers of Lishitz-Slyosov and Wagner [2, 3] in the late 60's, see also [4]. Coarsening is a general phenomena in which the natural size of a pattern increases with time in a continuous manner over a large range of time scales [5–8]. From a more applied point of view, coarsening has a significant impact on properties of matter such as the size of grains in polycrystalline solids, the hardening of metallic alloys, foam dynamics, sintering, sand dunes, etc. We focus here, on the fundamental aspect of coarsening of strained semiconductor quantum dots, such as the gallium-aluminum-nitride or silicon-germanium islands [9–21]. These islands are extensively under scrutiny both for their present and promising applications in electronics or optics, as for example single photons emitters, and for their insights into the fundamental processes of epitaxial growth. The properties and potential applications of quantum dot assembly are indeed crucially dependent on the amount of coarsening, that may critically affects the size homogeneity of such structures [20]. Moreover, the coarsening of such islands seems to be out of the classical description of Ostwald coarsening and requires more investigation.

The formation of self-organized semi-conductor quantum dots results from the Stranski-Krastanov growth mode [22]. In this scheme, growth initially proceeds as planar layers, that transform above a given critical thickness h_c , into islands separated by a wetting layer. These islands enable a partial relaxation of the elastic stress of the strained film, which overcomes capillary and wetting effects. In SiGe systems, this growth mode includes in

fact two different kinetic pathways. The seminal work of Lagally [23] showed that at large misfit—i.e. for a large enough Ge composition x , in a $\text{Si}_{1-x}\text{Ge}_x$ film, the island growth initiates via the nucleation of large enough fluctuations [24]. On the other hand, at low enough misfit (i.e. low enough x), further experiments [25, 26] revealed that the island growth begins with a nucleationless instability, reminiscent of the Asaro-Tiller-Grinfeld (ATG) instability [27–31]. In this case, the film becomes unstable above the critical height h_c , and an initial surface corrugation increases and transforms after some time into an assembly of quantum dots [25, 26, 32–38]. After its initial growth, the assembly of islands undergoes some coarsening, driven by the more efficient elastic relaxation of the largest islands. The initial roughly isotropic islands (prepyramids) thence ripen and, as they display steep enough slopes, they transform into anisotropic quantum dots of various sizes, especially pyramids and domes. Even in the paradigmatic SiGe systems, the nature of the islands coarsening is still a matter of debate and uncertainty [20]. For the initial isotropic islands [39–41], various theories predict a power-law evolution of the surface roughness and island density at constant mass (annealing), however the exponents of these power laws are clearly different from the classical Ostwald exponents [20]. In addition, the coarsening might be impacted by the growth dynamics [42], the anisotropy of the surface energy [43–49], alloying and compositional effects.

In the present article, we investigate analytically and numerically the basic but still challenging issue of the coarsening of strained islands in isotropic systems that results from the ATG instability. We have found that the island shape can be described by a simple analytical expression and we report the existence of a continuous family of solution for the island shape as a function of the system mass. Moreover we have found that the dynamics of coarsening of two islands can be reduced to a simple two step model. If the surface evolution might be well

*Electronic address: thomas.frisch@unice.fr

described initially in the framework of the linear theory of the ATG instability, the dynamics leads after some time to islands that require a non-linear analysis. The complexity of the dynamics describing the coarsening of such islands lies in the combination of out-of-equilibrium properties and of the long-range elastic effects. Furthermore, the power law behavior mentioned before arises in the late time dynamics where non-linear effects can not be neglected. We show here that this dynamics is intimately connected to the static equilibrium shapes of the islands and to the gradient of the chemical potential between two islands.

The article is organised as follows. In the first part, we describe the model under scrutiny that is a 1+1-dimensional strained film that evolves via surface diffusion. In the second part, we characterize analytically the stationary equilibrium solutions of our model. This solution corresponds to a single island sitting on top of a wetting layer, which characteristics (maximum height h_0 , surface (or mass) S , chemical potential μ) are analytically predicted. In particular, we show that the wetting interactions, yields the existence of a minimal island height. In the third part, we numerically integrate the evolution equation of a simple system composed by two islands with slightly different heights, which interaction leads to a single island after complete coarsening. In the last part, we derive an analytical model that describes the two-islands coarsening dynamics. We show that it is characterized by a two step evolution, with two specific time scales. The first step is well described by a quasi-static approach where each island chemical potential (whose gradient rules the mass transfer between them) is determined by the steady states values. It is associated with an exponential evolution of the islands heights, with a characteristic time scale t_c proportional to the chemical potential gradients, i.e. to the difference of the islands chemical potentials divided by their separating distance d . The second coarsening step occurs once the smallest island is smaller than the minimal stable island height, and therefore quickly dissolves on the wetting layer. It is associated with a second characteristic time scale τ that describes the dynamics of diffusion of a perturbation on a wetting layer, and that depends on the system size. This two-step dynamical evolution compares favorably with the direct numerical simulation of the coarsening dynamics. The two islands coarsening can be simply modelled by a system of differential equations for each island height. Conclusions and perspectives are drawn in the last part, where this study is promoted in perspective with the more general study of the coarsening of an assembly of islands.

I. CONTINUUM MODEL

We study a film-substrate system, made of a thin film lying on a substrate evolving only via surface diffusion. For studying the formation and the dynamics of the is-

land, we use a standard surface diffusion model which dynamics is governed by [30]:

$$\frac{\partial h}{\partial t} = \mathcal{D} \sqrt{1 + h_x^2} \frac{\partial^2 \mu}{\partial s^2}, \quad (1)$$

where \mathcal{D} is the surface diffusion coefficient, $\partial/\partial s$ the surface gradient and μ the chemical potential, that depends on the elastic and the surface energy. The upper film boundary is free and localized at $z = h(x)$, while the film/substrate interface at $z = 0$ is coherent. We solve the Lamé mechanic equilibrium equations with linear isotropic relations. For simplification, we assume that the film and substrate share the same elastic constants. When the film is flat $h(x) = cte$ it is subject to an elastic stress measured in unit of the volumetric elastic energy $\mathcal{E}_0 = E \eta^2 / (1 - \nu)$. Here $\eta = (a_f - a_s)/a_s$ is the misfit where a_f (resp. a_s) is the film (resp. substrate) lattice spacing, E is the Young's modulus, and ν the Poisson's coefficient. In the general case, when $h(x)$ displays small slopes, the mechanical equilibrium problem can be solved analytically [see e.g. [41]] and its solution is given in terms of the Hilbert transform \mathcal{H} of the surface profile. In addition, wetting interactions between the film and its substrate prove to be crucial in thin films. It might be describe by a height-dependant surface energy $\gamma(h)$ [39, 55–58]. In semiconductor systems, one can consider a smooth $\gamma(h)$ with the generic form characterized by a length δ , amplitude c_w and generic form $\gamma(h) = \gamma_f [1 + c_w f(h/\delta)]$, where $f(h \rightarrow \infty) = 0$. Here δ is of the order of the wetting layer (a few Angstroms). Adding the elastic and the capillary effects, one finds the chemical potential:

$$\mu(x) = \mathcal{E}[h] + \gamma(h) \frac{\partial^2 h}{\partial x^2} + \gamma'(h) / \sqrt{1 + h_x^2}, \quad (2)$$

where $\mathcal{E}[h]$ is the volumetric elastic energy on the surface and the third term in Eq. (2) is due to wetting where $\gamma'(h) = \frac{\partial \gamma}{\partial h}$. By balancing the elastic energy to the surface energy, we deduce the characteristic length $l_0 = \gamma_f / [2(1 + \nu)\mathcal{E}_0]$ describing the typical size of an horizontal surface undulation and the associated time scale $t_0 = l_0^4 / (\mathcal{D}\gamma_f)$. For example, for a $Si_{0.75}Ge_{0.25}$ film on Si, we find $l_0 = 27$ nm and $t_0 = 23$ s at 700 C (see [59] for an estimate of surface diffusion coefficients). In the small slope approximation, we obtain the following dimensionless equation for the surface evolution

$$\partial_t h = -\partial_{xx} \left[\partial_{xx} h + \frac{c_w}{\delta} e^{-h/\delta} + \mathcal{H}[\partial_x h] \right], \quad (3)$$

where $\mathcal{H}[\partial_x h]$ is the Hilbert transform of the spatial derivative of $h(x, t)$ defined as $\mathcal{F}^{-1}(|k|\mathcal{F}(h))$ where \mathcal{F} is the Fourier transform [41]. The first term in the r.h.s. Eq. (3) represents the stabilising effect of the surface energy, the second term is the wetting potential and the third term represents the destabilising effect of the elastic strain. Note that Eq. (3) represents a conservation equation, and the integral $\int h(x) dx$ (which represents the total amount of deposited material) is constant. This equation is non-linear, and we use a pseudo-spectral method

to solve it numerically [41]. Moreover, as we shall see, an analytical insight can be obtained from an analysis of the stationary solution of Eq. (3). As shown previously [41], there exists a critical height h_c above which a flat film becomes unstable with respect to infinitesimal perturbations,

$$h_c = -\delta \ln(\delta^2/4c_w). \quad (4)$$

For an initial height above h_c , the initial perturbation evolves towards an assembly of islands that display a non-interrupted coarsening [41] leading to one stationary island. We describe analytically the characteristics of such a stationary island in next Section.

II. THE STATIONARY ISLAND

The goal of this section is to study the equilibrium stationary solutions of Eq. (3), and in particular the island profile. Indeed, above the critical height h_c , the evolution of the surface is characterized by a non-interrupted coarsening that eventually leads to a one-island solution [41]. This stationary profile is given by one island of height h_0 lying on top of a wetting layer of thickness h_w , see Fig 1. It is characterized by a constant chemical potential μ on the surface,

$$\mu = -\partial_{xx}h - \frac{c_w}{\delta}e^{-h/\delta} - \mathcal{H}[\partial_x h]. \quad (5)$$

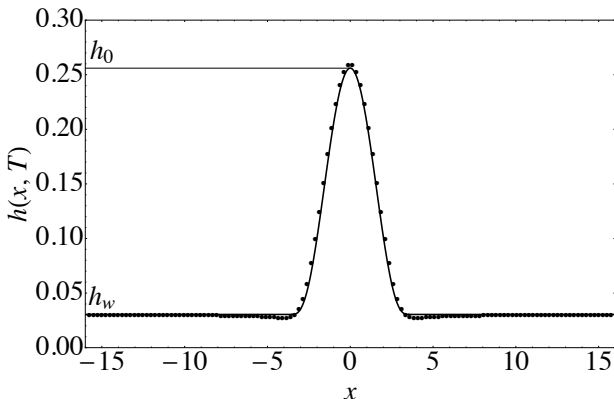


FIG. 1: Island like solution resulting from the long time evolution of an initially small surface perturbation. The dots are the stationary profile obtained with numerical simulation of Eq. (3). The system size is $L = 32$, $c_w = 0.045$ and $\delta = 0.005$. The time is $T = 1000$. The horizontal and vertical axis are in units of l_0 . The line is the *ansatz* given in Eq. (6), with a width $W = 9\pi/4$. The value of h_0 is taken from top of the island and the corresponding value of h_w is obtained from Eq. (7). The value of the area $S = \int_{-L/2}^{L/2} h(x, t) dx = 1.5$ is conserved throughout the dynamics.

The stationary island characteristics maximum height h_0 and width W , can be predicted by the use of a simple model. This model has a no free parameters and

can be characterised by the total surface of the system $S = \int_{-L/2}^{L/2} h(x, t) dx$ with L the system size. Thus islands of different height h_0 can be generated numerically by varying the control parameter S in the initial condition. Motivated by the result of the numerical simulation of

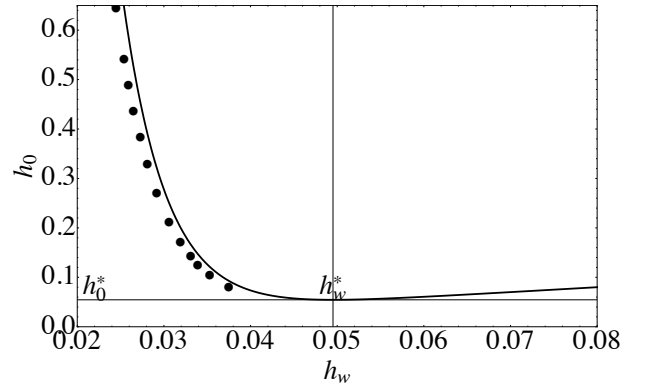


FIG. 2: Height of the island h_0 as a function of h_w in units of l_0 . Dots are obtained by simulations of Eq. (3) and the full line is the *ansatz* given in Eq. (6). The value of h_0^* is defined on the figure. The different point are obtained by performing different simulations for different value of the initial surface S . The value of the parameters L , c_w and δ are the same then the one used in Fig. 1. The minimal value of h_0^* will be defined in Eq. (8)

Eq. (3), we choose the following *ansatz* for the stationary solution of Eq. (3). For $|x| < W/2$

$$h(x) = (h_0 - h_w) \left(\frac{2}{W} \right)^6 \left[\left(\frac{W}{2} \right)^2 - x^2 \right]^3 + h_w, \quad (6)$$

while for $|x| > W/2$, we choose $h(x) = h_w$. This *ansatz* satisfies the continuity of the function at $|x| = W/2$ and of its derivatives up to third order and is characterized by three parameters. After substitution of this *ansatz* in Eq. (5), and using a simple polynomial expansion around the point $x = 0$ up to second order in x , we obtain at order x^0 the following relation between the island height h_0 and the height of the wetting layer h_w :

$$h_0 = h_w + \frac{135\pi^2}{128} \frac{c_w}{\delta} e^{-h_w/\delta}. \quad (7)$$

At order x^2 , we obtain the relation for the width of the island $W = \frac{9\pi}{4}$ [60].

In Fig. 1, we compare the profile of a stationary island obtained by numerical simulation of Eq. (3) with this *ansatz*. The agreement between the two is rather good with small discrepancies located on a small zone at the foot of the island [61].

We also plot in Fig. 2 the height of the island h_0 at equilibrium as a function of the height of the wetting layer far away of the island h_w . The simulation values

are obtained by varying the system surfaces (S) while the *ansatz* result follows from Eq. (7). Again, the agreement is rather good. Of special interest is the fact that h_0 has a minimal value called h_0^* . The critical height h_0^* is defined by the relation $\frac{\partial h_0}{\partial h_w} = 0$, this leads using Eq. (7) to the result:

$$h_0^* = \delta \left[1 + \ln \left(\frac{c_w 135 \pi^2}{\delta^2 128} \right) \right], \quad (8)$$

while the associated wetting thickness is:

$$h_w^* = \delta \ln \left(\frac{c_w 135 \pi^2}{\delta^2 128} \right). \quad (9)$$

As we observed numerically, islands with h_0 smaller than h_0^* are not stable. Hence, the presence of wetting interactions enforce the existence of minimal value of the equilibrium island surface, in addition to the existence of a minimal film thickness h_c . The critical island height could be observed experimentally and it will be important in the description of the coarsening process.

As regards to the chemical potential, each island-like stationary solutions of Eq. (5) is defined by

$$\mu_i = -\frac{c_w}{\delta} e^{-h_w/\delta}. \quad (10)$$

This results comes from the fact that far from the island the film is rather flat so that h_x and h_{xx} vanish and only the wetting potential term remains dominant in Eq. (5). Therefore the simple knowledge of h_w can leads to the determination of the chemical potential and reciprocally. Using Eqs. (9) and (10), we find that the critical chemical potential μ^* associated with the critical solution with h_0^* reads

$$\mu^* = -\delta \frac{128}{135 \pi^2}. \quad (11)$$

We mentioned previously that islands are uniquely characterised by the surface S . Now that we have the profile of the island given in Eq. (6), we can calculate its the surface S ,

$$S = h_w L + \frac{243 \pi^3}{224} \frac{c_w}{\delta} e^{-h_w/\delta} \equiv \langle h \rangle L. \quad (12)$$

The total surface (mass) S can thus be varied by varying the mean height $\langle h \rangle$ or the size L of the system.

We plot in Fig. 3, the island maximum height h_0 and the height of the wetting layer h_w versus the surface S by varying $\langle h \rangle$. As expected, we observe in Fig. 3 that the maximum height of the island increases as the surface S increase. As h_0 is a decreasing function of h_w , see Fig. 2, we also find that h_w is decreasing function of the island surface S as shown in the inset of Fig. 3. This may be associated with the larger relaxation of the larger islands that are in equilibrium with a more stable thin wetting layer.

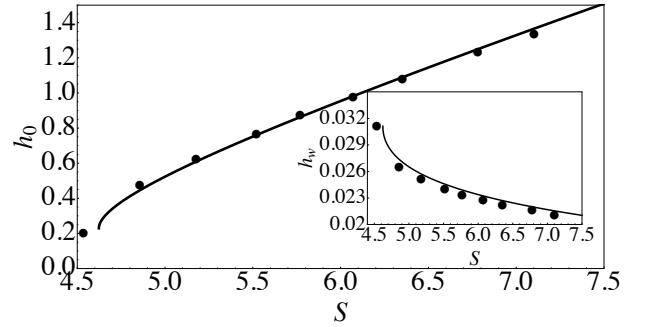


FIG. 3: The height h_0 as a function of the surface $S = \langle h \rangle L$ with L being fixed. The horizontal and vertical axis are in units of l_0^2 and l_0 respectively. The dots are obtained by numerical simulation of Eq. (3). The curve corresponds to Eq. (12) and Eq. (7). The inset is the height h_w as a function of S . The system size is $L = 128$, $c_w = 0.045$ and $\delta = 0.005$.

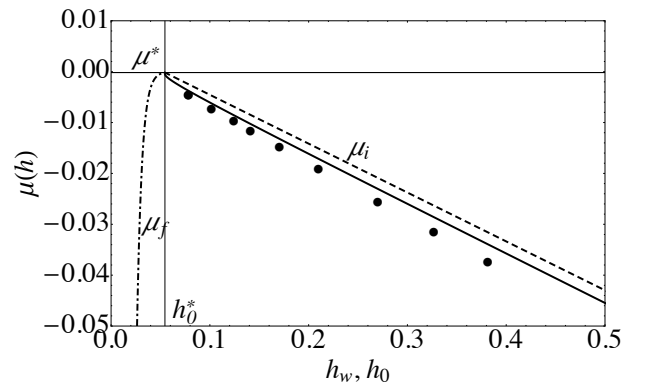


FIG. 4: For $h < h_0^*$, the dash-dotted line is the chemical potential $\mu = -\frac{c_w}{\delta} e^{-h/\delta}$ as a function height for the flat film. The unit of the vertical axis is in $\mathcal{E}_0 = E \eta^2 / (1 - \nu) = 6.7 * 10^7 \text{ Joules/m}^3$ and the unit of the horizontal axis is in l_0 . For $h > h_0^*$, the horizontal axis $h = h_0$. The dots represent the numerical simulation for the equilibrium state of an island given by Eq. (3). The continuous curve is the prediction given using Eq. (7) and Eq. (10) for the chemical potential of the island. The dashed curve is given by Eq. (13).

We now study the chemical potential associated with the one island solution. For $h_0 \geq h_0^*$, there exists an equilibrium island solution. Its chemical potential is given by Eq. (10) in terms of the wetting layer thickness h_w . The equilibrium island chemical potential is plotted as a function of h_0 in Fig. 4. As the island surface increases, hence h_0 increases, the island chemical potential naturally decreases, showing the larger elastic relaxation of large islands. This conclusion was also found in the three-dimensional island under study in [41]. When $h_0 < h_0^*$, only the flat film solution exists, its chemical potential is entirely given by Eq. (11). We also plot this chemical potential as a function of h_w as enforced by the (attractive) wetting interactions. At equilibrium, for $h > h_c$, an island of

thickness h_0 coexist with a wetting layer of thickness h_w , that have the same chemical potential. In Fig 4, we again find a good agreement between the numerical simulation and our theoretical prediction. As expected the chemical potential has a maximum value μ^* , given by Eq. (11), associated with the minimal value of the surface height h_0^* . The dashed curve in Fig. 4 represents the linear approximation to μ_i ,

$$\mu_i^l \simeq -c(h_0 - h_0^*) + \mu^*, \quad (13)$$

that has been obtained using Eq. (7) and Eq. (10), here $c = \frac{128}{135\pi^2}$.

III. COARSENING OF TWO ISLANDS

We now address the question of coarsening of two islands of slightly different amplitudes (heights) separated by a distance d . Let h_1 and h_2 be the height for the small and large islands respectively (left peak and right peak on Fig. 5). These quantities will evolve with time. In Fig. 5, we represent the time evolution of the two islands as enforced by the dynamical evolution Eq. (3). The initial condition is given by two islands at equilibrium with amplitude $h_1 = h_i - \epsilon$ and $h_2 = h_i + \epsilon$. We find a first regime where the height of the small island decreases while the height of the large island increases. Then, the small island reaches the critical height h_0^* at time t_c (Fig. 5.d). In the second regime for $t > t_c$ (Fig. 5.e), the remaining mass in the wetting layer diffuses towards the larger island, which relaxes towards its equilibrium state (Fig. 5.f). The largest island height h_2 constantly increases during the whole coarsening process.

In Fig. 6, we plot the temporal evolution of the local chemical potential associated with the evolution given by Eq. (3). The chemical potential on the small island increases when its height decreases as it becomes less and less stable, and conversely for the large island. Before t_c , the chemical potential μ between the two islands is a linear decreasing function of space as shown for example in Fig. 6.b and Fig. 6.c. Furthermore, when $t < t_c$, and outside the islands, the chemical potential has variations on the scale of the system L . It is due to finite size effects that can be neglected as long as $d \ll L$. When the critical height of the small island is reached (Fig. 6.d) at time $t = t_c$, the chemical potential of the small island is equal to μ^* and the height of the small island h_1 is h_0^* . For $t > t_c$, while h_2 is growing, the diffusion on the wetting layer takes place on a scale of the order L . This second regime relaxes towards equilibrium, where finally the chemical potential is constant, Fig. (6.f).

IV. MODEL OF COARSENING

We now develop a simple mean-field model that describes the coarsening phenomena in two stages. In this

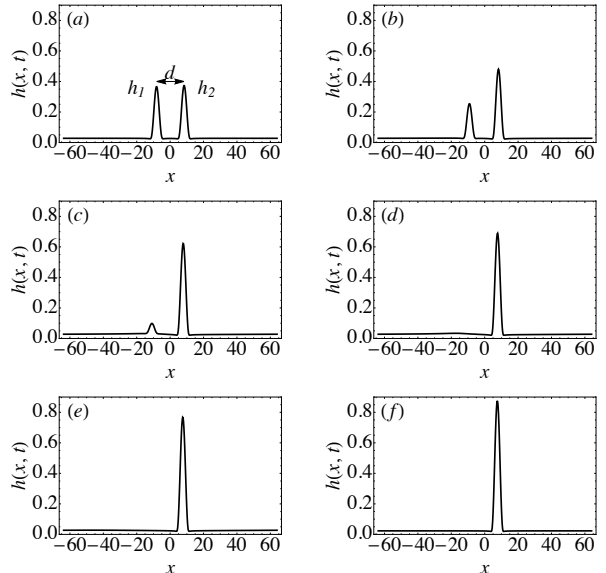


FIG. 5: Numerical resolution of Eq. (3) for the profile evolution of two interacting islands separated by a distance d . The horizontal and vertical axis are in units of l_0 . The system size is $L = 128$. The initial condition consists of two islands separated by a distance $d = 16$ and initial amplitudes $h_1 = 0.36$ (left island) and $h_2 = 0.37$ (right island) with time a) $t = 0$, b) $t = 700$, c) $t = 1080$ before t_c , d) characteristic time $t = t_c = 1350$, e) $t = 1550$ and f) $t = 2580$ when the equilibrium state is reached.

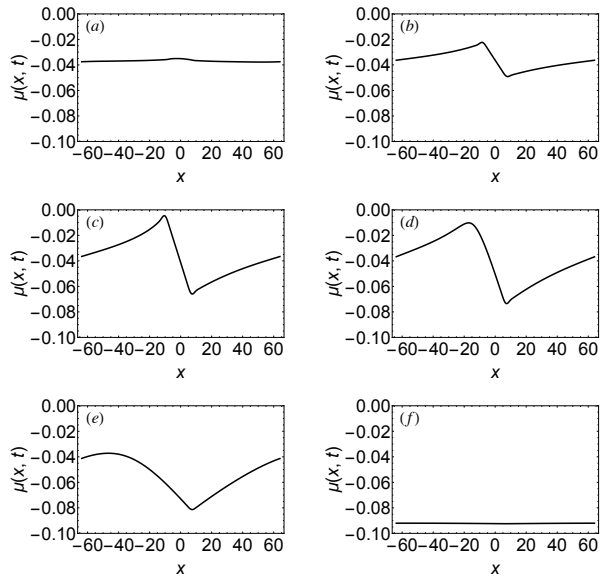


FIG. 6: Numerical evolution of Eq. (3) for the chemical potential of two interacting islands corresponding to Fig. 5. The unit of the vertical axis is $\mathcal{E}_0 = 6.7 \times 10^7 \text{ Joules/m}^3$. The horizontal axis is in unit of l_0 .

model the islands are represented by a punctual object of varying surface. The advantage of this model is that

it requires only a small number of input parameters such as the width of the island W and the chemical potential difference between the two islands. We make the assumption that the dynamics is close to equilibrium so that the results for stationary island can be exploited. The first coarsening stage is defined for $t < t_c$ when the two islands co-exist while for $t > t_c$, the smaller island has disappeared and perturbation of the wetting layer diffuses towards the larger island.

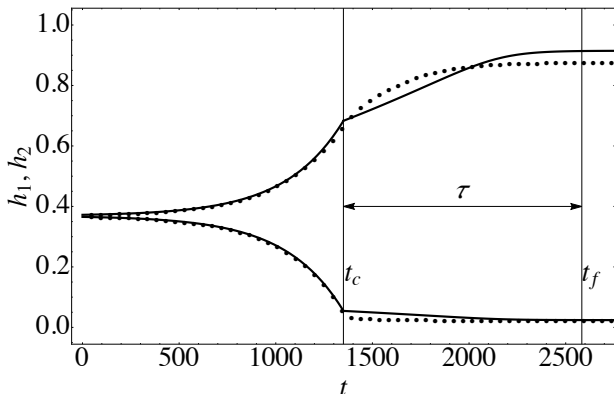


FIG. 7: Amplitude h_1 and h_2 of the islands as a function of time. Full curves are the theoretical prediction and the dashed curve is the numerical simulation. The times t_c and t_f are represented on the figure. τ is defined as the time since t_c for which the amplitude h_2 of the large island has reach 0.99 of its equilibrium value. The horizontal and vertical axis are in units of t_0 and l_0 respectively.

For $t < t_c$, we model the dynamics of the height of each island based on the flux of matter induced by the chemical potential gradient between the two islands. This spatial gradient takes place on a length scale of order d . Mass conservation enforces in this approximation [62]

$$\begin{aligned} \alpha W \partial_t h_1 &= \frac{\mu_i(h_2) - \mu_i(h_1)}{d} \\ \alpha W \partial_t h_2 &= \frac{\mu_i(h_1) - \mu_i(h_2)}{d} \end{aligned} \quad (14)$$

where h_1 is the height of the small island, h_2 the height of the large one, W their width and α a constant geometrical factor which is of order one [63].

Furthermore, we assume in the following that the island chemical potential might be given by the linear form given in Eq. (13) Hence, the system (14) simplifies into

$$\begin{aligned} \alpha W \partial_t h_1 &= -\frac{c(h_2 - h_1)}{d} \\ \alpha W \partial_t h_2 &= -\frac{c(h_1 - h_2)}{d} \end{aligned} \quad (15)$$

where $c = \frac{128}{135\pi^2}$, given by the slope of Eq. (13). Let us write the amplitude of the islands

$$\begin{aligned} h_1(t) &= h_i - \epsilon \tilde{h}(t) \\ h_2(t) &= h_i + \epsilon \tilde{h}(t) \end{aligned} \quad (16)$$

which implies that $h_1(t) + h_2(t) = 2h_i$ and \tilde{h} is the perturbation of the stationary state. Solving (15), we deduce

that the perturbation increase exponentially

$$\tilde{h}(t) = e^{\frac{2c}{d\alpha W} t}, \quad (17)$$

in the first temporal regime. This regime extends up to t_c , such as $h_1(t_c) = h_0^*$ which leads to $h_0^* = h_i - \epsilon e^{\frac{2c}{d\alpha W} t_c}$. Hence, we find

$$t_c = \frac{d\alpha W}{2c} \ln \left[\frac{h_i - h_0^*}{\epsilon} \right]. \quad (18)$$

As shown on Fig. 7, there is a good agreement between the numerical simulation and this estimate.

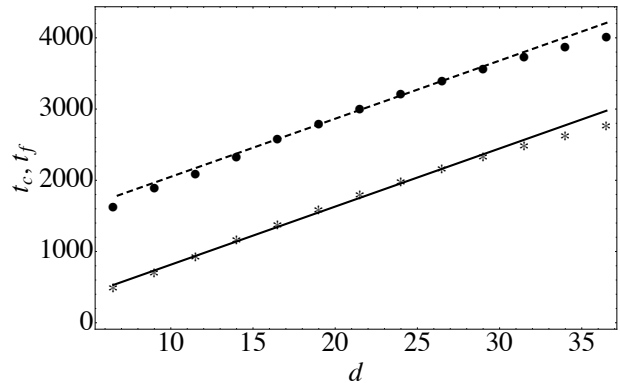


FIG. 8: Characteristic times t_c and t_f (* and • respectively), as a function of the distance d between the islands, obtained by numerical simulation. The line is t_c from Eq. (18) and the dashed line is the $t_f + \tau$, where τ is obtained with the numerical solution of Eq. (21). The system size is $L = 128$. The time t_f for the disappearance of the two islands increases with the system size, it is linear when $d/L \ll 1$. When d increases and becomes of the order of L there are deviation from the linear law due to the effect of the periodic boundary conditions. The horizontal and vertical axis are in units of l_0 and t_0 respectively.

The second regime is reached when the amplitude of the small island becomes smaller than the critical height h_0^* , $h_1 < h_0^*$ at $t > t_c$. Mass diffusion then occurs on the wetting layer. The characteristic time τ of this second regime then depends essentially on the full size of the system L and only weakly on the distance d . To quantify, we write the mass conservation equation as

$$\beta(L - W)h_1 + \alpha W h_2 = S, \quad (19)$$

where α and β are geometrical factors respectively for the island and for the wetting layer while S is fixed by the initial conditions. From this relation, we deduce that

$$\partial_t h_1 = -A \partial_t h_2 \quad \text{here} \quad A = \frac{\alpha W}{\beta(L - W)}. \quad (20)$$

Again, we have assumed that the growth rate of the island is proportional to the gradient of chemical potential. This gradient occurs on a scale of order L so that

$$\alpha W \partial_t h_2 = \frac{2[\mu_f(h_1) - \mu_i^l(h_2)]}{L}. \quad (21)$$

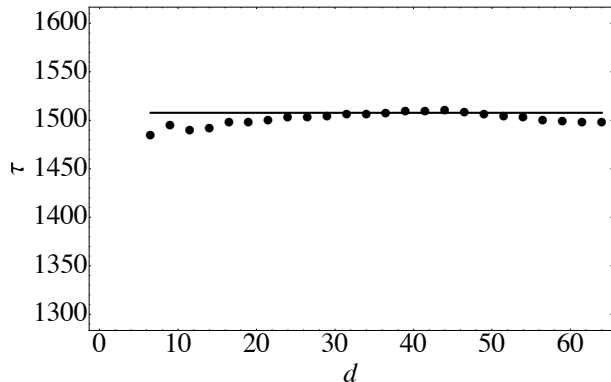


FIG. 9: Characteristic time τ as a function of the distance d between the islands, obtained by numerical simulation of Eq. (3). The line is the time τ obtained with the solution of Eq. (21). The horizontal and vertical axis are in units of l_0 and t_0 respectively.

Here $\mu_f(h_1) = -\frac{c_w}{\delta} e^{-h_1/\delta}$ is the approximate wetting chemical potential of the wetting layer. In order to obtain the time evolution of $h_1(t)$ and $h_2(t)$, we have integrated numerically Eqs. (20,21). As shown on Fig. 7, the system of Eqs. (20,21) captures well the numerical evolution of Eq. (3). The amplitude of the island increases with time before saturating at a value close to the predicted value which depends on the value of S as shown in Fig 3.

In order to quantify this coarsening process, we define the time t_f as the time at which the amplitude of the large island has reached 0.99 of its equilibrium value. In addition, we define τ such as $t_f = (\tau + t_c)$.

In Fig. 8, we plot the different times t_c and t_f as a function of the distance d between the islands using the numerical and the analytic results Eq. (18). We observe, as long as d/L is small, that t_c increases linearly with the distance d as predicted by Eq. (18). When d increases and becomes of the order of L there are deviation from the linear law in d due to the image interaction since our numerical simulation are performed in a periodic system. In Fig. 9, we show that the time τ is almost independent of the distance d separating the islands. As a conclusion, Figs. 8 and 9 show that τ is independent of d while t_f and t_c increase linearly with d .

V. CONCLUSION AND PERSPECTIVES

We have studied in this article the dynamics and the coarsening of strained islands. We first obtained an ap-

proximate analytical equation for a stationary island lying on a wetting layer. This approach allows to predict the width W of the island and to relate the island amplitude to the height of the wetting layer. We have shown that the presence of the wetting potential leads to the existence of a critical island height h_0^* below which the island does not exist. The comparison between the approximate analytical solution and the stationary state resulting from the numerical integration of the mass diffusion equation is good. Secondly, we have investigate the dynamics of coarsening of two islands and we have found that this coarsening is non-interrupted, the small island disappears in favour of the largest one. As observed numerically, in a first regime the height of the largest island increases exponentially until a time t_c at which the smallest island becomes unstable. The characteristic time t_c scales like the distance d between the islands. In a second regime, which lasts a time τ , the perturbation on the wetting layer diffuses and the amplitude of the remaining island grows until it reaches its equilibrium value. This second regime is quite independent of the distance d between the initial island. In order to model this dynamics, we propose a simple model based on a quasi-static hypothesis with mass currents driven by the gradient of the chemical potential. These results pave the way for a description of coarsening in strained systems with long-range interactions. We will extend this analysis to the problem of coarsening of an array of N islands as generated by the Asaro-Tiller-Grinfeld instability by generalizing the set of Eqs. (14) to N islands. An extension of this analytical work on three dimensional islands with inclusion of the surface energy anisotropy will be considered in the future.

Acknowledgments

We would like to thank Pierre Müller, Julien Brault, Benjamin Damilano, Philippe Vennéguès, Matthieu Leroux, Jean Massies, Franck Celestini, Jean Rachenbach, Isabelle Berbezier and Alberto Verga for useful discussion. We thank the ANR NanoGanUV for financial support.

-
- [1] W. Ostwald, Lehrbuch der Allgemeinen Chemie **2**, 280 (1896).
 - [2] I. Lishitz and V. Slyosov, J. Phys. Chem. Solids **1961**,

35 (1961).

- [3] C. Wagner, Theorie der Alterung von Niederschlagen durch Umlasen (Ostwald-Reifung) **65**, 581 (1961).

- [4] J. A. Marqusee, J. Chem. Phys. **81**, 976 (1984).
- [5] P. Politi, G. Grenet, A. Marty, A. Ponchet, and J. Villain, Physics Reports **324**, 271 (2000).
- [6] L. Ratke and P. W. Voorhees, *Growth and Coarsening* (Springer Berlin Heidelberg, 2002).
- [7] C. Misbah, O. Pierre-Louis, and Y. Saito, Rev. Mod. Phys. **82**, 981 (2010).
- [8] S. Biagi, C. Misbah, and P. Politi, Phys. Rev. Lett. **109**, 096101 (2012).
- [9] J. Stangl, V. Holý, and G. Bauer, Rev. Mod. Phys. **76**, 725 (2004).
- [10] J. L. Gray, R. Hull, P. Lam, C.-H. Sutter, J. Means, and J. A. Floro, Phys. Rev. B **72**, 155323 (2005).
- [11] J.-M. Baribeau, X. Wu, N. L. Rowell, and D. J. Lockwood, J. Phys.: Condens. Matter **18**, R139 (2006).
- [12] Y. Tu and J. Tersoff, Phys. Rev. Lett. **98**, 096103 (2007).
- [13] M. R. McKay, J. A. Venables, and J. Drucker, Solid State Commun. **149**, 1403 (2009).
- [14] I. Berbezier and A. Ronda, Surf. Sci. Rep. **64**, 47 (2009).
- [15] M. Brehm, F. Montalenti, M. Grydlik, G. Vastola, H. Lichtenberger, N. Hrauda, M. J. Beck, T. Fromherz, F. Schäffler, L. Miglio, et al., Phys. Rev. B **80**, 205321 (2009).
- [16] J. Brault, T. Huault, F. Natali, B. Damilano, D. Lefebvre, M. Leroux, M. Korytov, and J. Massies, Journal of Applied Physics **105**, 033519 (2009).
- [17] F. A. Zwanenburg, A. S. Dzurak, A. Morello, M. Y. Simmons, L. C. L. Hollenberg, G. Klimeck, S. Rogge, S. N. Coppersmith, and M. A. Eriksson, Rev. Mod. Phys. **85**, 961 (2013).
- [18] J.-M. Baribeau, X. Wu, N. L. Rowell, and D. J. Lockwood, J. Phys.: Condens. Matter **18**, R139 (2006).
- [19] D. D. Vvedensky, *Oxford Handb Nanosci Technol* (ed. A. V. Narlikar and Y. Y. Fu, Oxford University Press, Oxford, England, 2010), vol. 3, chap. Quantum Dots: Self-organized and self-limiting structures, p. 205.
- [20] J.-N. Aqua, I. Berbezier, L. Favre, T. Frisch, and A. Ronda, Phys. Rep. **522**, 59 (2013).
- [21] J.-N. Aqua, A. Gouyé, A. Ronda, T. Frisch, and I. Berbezier, Phys. Rev. Lett. **110**, 096101 (2013).
- [22] I. N. Stranski and L. Krastanov, Ber. Akad. Wiss. Wien, Mater., Math.-Nat. Kl. IIB **146**, 797 (1938).
- [23] Y. W. Mo, D. E. Savage, B. S. Swartzentruber, and M. G. Lagally, Phys. Rev. Lett. **65**, 1020 (1990).
- [24] D. J. Eaglesham and M. Cerullo, Phys. Rev. Lett. **64**, 1943 (1990).
- [25] P. Sutter and M. G. Lagally, Phys. Rev. Lett. **84**, 4637 (2000).
- [26] R. M. Tromp, F. M. Ross, and M. C. Reuter, Phys. Rev. Lett. **84**, 4641 (2000).
- [27] R. J. Asaro and W. A. Tiller, Metall. Trans. **3**, 1789 (1972).
- [28] M. A. Grinfeld, Sov. Phys. Dokl. **31**, 831 (1986).
- [29] D. J. Srolovitz, Acta Metall. **37**, 621 (1989).
- [30] B. J. Spencer, P. W. Voorhees, and S. H. Davis, Phys. Rev. Lett. **67**, 3696 (1991).
- [31] P. Müller and A. Saúl, Surface Science Reports **54**, 157 (2004).
- [32] A. G. Cullis, D. J. Robbins, A. J. Pidduck, and P. W. Smith, J. Cryst. Growth **123**, 333 (1992).
- [33] D. E. Jesson, S. J. Pennycook, J.-M. Baribeau, and D. C. Houghton, Phys. Rev. Lett. **71**, 1744 (1993).
- [34] C. S. Ozkan, W. D. Nix, and H. Gao, Appl. Phys. Lett. **70**, 2247 (1997).
- [35] I. Berbezier, B. Gallas, A. Ronda, and J. Derrien, Surf. Sci. **412**, 415 (1998).
- [36] H. Gao and W. Nix, Annu. Rev. Mater. Sci. **29**, 173 (1999).
- [37] B. J. Spencer and J. Tersoff, Phys. Rev. Lett. **79**, 4858 (1997).
- [38] J. A. Floro, E. Chason, L. B. Freund, R. D. Twisten, R. Q. Hwang, and G. A. Lucadamo, Phys. Rev. B **59**, 1990 (1999).
- [39] Y. Pang and R. Huang, Phys. Rev. B **74**, 075413 (2006).
- [40] M. S. Levine, A. A. Golovin, S. H. Davis, and P. W. Voorhees, Phys. Rev. B **75**, 205312 (2007).
- [41] J.-N. Aqua, T. Frisch, and A. Verga, Phys. Rev. B **76**, 165319 (2007).
- [42] J.-N. Aqua, T. Frisch, and A. Verga, Phys. Rev. E **81**, 021605 (2010).
- [43] J.-N. Aqua, A. Gouyé, T. Auphan, T. Frisch, A. Ronda, and I. Berbezier, Appl. Phys. Lett. **98**, 161909 (2011).
- [44] M. Kästner and B. Voigtländer, Phys. Rev. Lett. **82**, 2745 (1999).
- [45] M. R. McKay, J. A. Venables, and J. Drucker, Phys. Rev. Lett. **101**, 216104 (2008).
- [46] J.-N. Aqua and T. Frisch, Phys. Rev. B **82**, 085322 (2010).
- [47] J.-N. Aqua, A. Gouyé, A. Ronda, T. Frisch, and I. Berbezier, Phys. Rev. Lett. **110**, 096101 (2013).
- [48] G. Medeiros-Ribeiro, T. I. Kamins, D. A. A. Ohlberg, and R. S. Williams, Mater. Sci. Eng. B **67**, 31 (1999).
- [49] V. A. Shchukin, D. Bimberg, T. P. Munt, and D. E. Jesson, Phys. Rev. Lett. **90**, 076102 (2003).
- [50] F. M. Ross, J. Tersoff, and R. M. Tromp, Phys. Rev. Lett. **80**, 984 (1998).
- [51] A. Rastelli, M. Stoffel, J. Tersoff, G. S. Kar, and O. G. Schmidt, Phys. Rev. Lett. **95**, 026103 (2005).
- [52] M. Stoffel, A. Rastelli, J. Stangl, T. Merdzhanova, G. Bauer, and O. G. Schmidt, Phys. Rev. B **75**, 113307 (2007).
- [53] X. Xu, J.-N. Aqua, and T. Frisch, J. Phys. : Condens. Matter **24**, 045002 (2012).
- [54] J. N. Aqua and X. Xu, Phys. Rev. E **90**, 030402 (2014).
- [55] P. Müller and R. Kern, Applied Surface Science **102**, 6 (1996).
- [56] B. J. Spencer, Phys. Rev. B **59**, 2011 (1999).
- [57] A. A. Golovin, S. H. Davis, and P. W. Voorhees, Phys. Rev. E **68**, 056203 (2003).
- [58] P. Müller and R. Kern, Surface Science **529**, 59 (2003).
- [59] E. Chason, J. Tsao, K. Horn, S. Picraux, and H. Atwater, Journal of Vacuum Science & Technology A **8**, 2507 (1990).
- [60] The calculation of the Hilbert transform is done in real space using the standard definition of the principal value integral.
- [61] These discrepancy can be improved by using higher order polynomial or matching methods between the wetting layer and the islands. However, an improvement of the solution does not lead to any qualitative change
- [62] For simplicity, we neglect finite size effects which lead to small terms in d/L due to the presence of periodic boundary conditions.
- [63] $\alpha = \int_{-W/2}^{W/2} h(x)dx/h_0W = 0.4636$ and $\beta = 0.22$.